ELSEVIER

Physica E 5 (2000) 196–199

PHYSICA E

www.elsevier.nl/locate/physe

Electron–plasmon resonance in quantum wells with inverted subband population

Mikhail Kisin[a, *], Michael Stroscio[b], Gregory Belenky[a], Serge Luryi[a]

[a] *Department of Electrical Engineering, SUNY at Stony Brook, NY 11794, USA*
[b] *US Army Research Office, P.O. Box 12211, Research Triangle Park, NC 27709, USA*

Received 14 January 1999; accepted 2 September 1999

Abstract

The inverted order of subband occupation, $n_2 > n_1$, in quantum-well heterostructures designed for the intersubband lasers results in a novel effective relaxation mechanism for nonequilibrium electrons in the lower subband due to emission of the intersubband plasmons. In contrast to the cascade relaxation by phonons and intrasubband plasmons, this one-step scattering process efficiently fills the final states for light-emitting transitions. Resonant screening, which is influenced by the process of intersubband plasmon excitation, leads to downshift and narrowing of the intersubband optical emission spectra.

PACS: 71.45.−d; 72.10.−d; 78.66

Keywords: Semiconductor heterostructures; Electron relaxation; Plasmons; Phonons

At low 2D-electron concentrations, the relaxation processes in A3B5 quantum wells are determined basically by LO–phonon emission. The optical-phonon spectrum of the heterostructure is significantly modified by the presence of the interfaces and includes interface and confined modes. In narrow quantum wells, the antisymmetric interface mode, $\hbar\omega_{\mathrm{ph}}^{\mathrm{A}}$, dominates the intersubband electron relaxation [1,2]. At the level of electron concentrations $N_{\mathrm{s}} \geqslant 10^{11}$ cm^{-2} plasmon-like branch of the spectrum of coupled plasmon–phonon polar excitations becomes equally important for the electron relaxation [3]. The plasmon spectrum in a quantum well is also modified and consists of low-energy intrasubband and high-energy intersubband excitations [4]. The intersubband plasmon mode, being characterized by an antisymmetric potential distribution, could participate in the intersubband relaxation causing electron intersubband 2–1 transitions with a small momentum transfer q. However, for the normal ordering of subband filling, when most of electrons occupy the lower subband states, $N_{\mathrm{S}} \approx n_1$, $k_1 \leqslant k_{\mathrm{F}}$, this kind of transition becomes possible only for high-energy electrons in the second subband $\varepsilon_2 \geqslant \varepsilon_{\mathrm{th}} \approx \varepsilon_{\mathrm{F}} + \delta$ because of the up-shift δ of the energy of the intersubband

* Corresponding author. Tel.: 516-632-8421; fax: 516-632-8494.
E-mail address: mvk@ee.sunysb.edu (M. Kisin)

1386-9477/00/\$ - see front matter
PII: S1386-9477(99)00254-4

plasmons [5]:

$$\hbar\omega_{\rm pl}^{\rm A+}(q) \approx \Delta_{21} + \delta, \quad \delta(q \ll k_{\rm F}) \approx \frac{e^2 N_{\rm s} S}{\kappa_0 \kappa}. \tag{1}$$

Here S is the depolarization integral, κ is the dielectric constant, and $k_{\rm F}$ and $\varepsilon_{\rm F}$ are Fermi wave vector and energy.

In a system with normal subband occupation the intersubband plasmon excitation *raises* the system energy from the ground state energy E_0 by quantum $\hbar\omega_{\rm pl}^{\rm A+}$. In contrast, the polarization of the nonequilibrium system with inverse population $N_{\rm S} \approx n_2$ due to the intersubband plasmon excitation leads to the *lowering* of the energy of the initial state by the quantum $\hbar\omega_{\rm pl}^{\rm A-} \approx \Delta_{21} - \delta$, since the intersubband plasmon potential admixes the lower-energy states from the first subband to the occupied second subband states. As a result, the scattering process with intersubband plasmon emission in the inverted system must include the intersubband 1–2 electron transition associated with the absorption of the de-excitation energy $\hbar\omega_{\rm pl}^{\rm A-}$. For this scattering process, the initial and final state energies, $E_{\rm i} = E_0 + \varepsilon_1(k)$ and $E_{\rm f} = E_0 + \Delta_{21} + \varepsilon_2(\boldsymbol{k} - \boldsymbol{q}) - \hbar\omega_{\rm pl}^{\rm A-}(q)$, are related by the conservation law, which imposes the same threshold for the allowed kinetic energy ε_1 of scattered electrons, viz. $\varepsilon_1 \geqslant \varepsilon_{\rm th} \approx \varepsilon_{\rm F} + \delta$. In random phase approximation, the state of the inverted system with one excited intersubband plasmon can be represented as $|E_0 - \hbar\omega_{\rm pl}^{\rm A-}(q)\rangle = \sum F(k)\hat{c}^{+}_{1,\boldsymbol{k}+\boldsymbol{q}}\hat{c}_{2,\boldsymbol{k}}|E_0\rangle$. The expectation value of the first-subband number operator in this state is then $\langle \hat{c}^{+}_{1,\boldsymbol{k}}\hat{c}_{1,\boldsymbol{k}}\rangle = |F(\boldsymbol{k}+\boldsymbol{q})|^2$, where the form-factor $F(k)$ obeys the normalization condition $\sum |F(k)|^2 = 1$. This implies an effective increase of the first subband occupation by one electron. Since $q \ll k_{\rm F}$ this process fills the bottom states of the first subband – to a good approximation uniformly.

In Fig. 1 we show the spectrum of electron excitation in a two-subband system with normal (a) and inverted (b) ordering of subband occupation. The continuum single-particle excitations of the initial state E_0 is represented by shaded regions and the dispersions of intrasubband (11), (22) and intersubband (12), (21) collective excitations are shown by heavy solid lines. Dashed lines illustrate the scattering of an external electron $\boldsymbol{e}$ by an intersubband plasmon. In the insets we show electron–electron scattering events which are analogous to the electron–

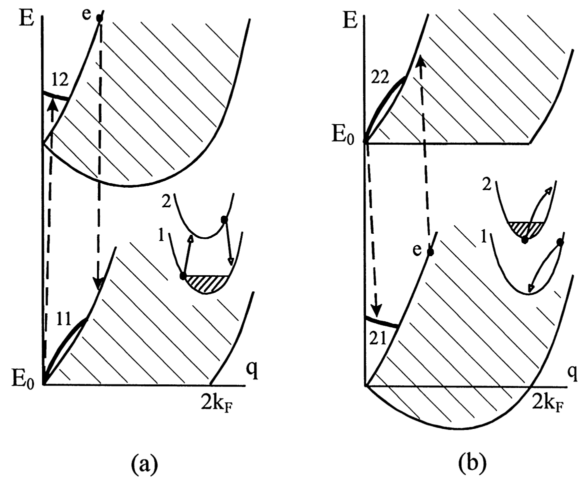

Fig. 1. Spectrum of electron excitation in a two-subband system with normal (a) and inverted (b) ordering of subband occupation.

plasmon processes but are ineffective due to electron wave function orthogonality (a) or large momentum transfer (b).

Consider now the simplest model of intrasubband relaxation for nonequilibrium high-energy electrons coming to subband 1 from subband 2 after the emission of an optical phonon [6,7]. We suppose the depopulation time of the first subband, $\tau_{1\rm out}$, be fast enough, so that in a steady state one has $n_1 \ll n_2$. Then, the electron–plasmon scattering rates are determined essentially by the electron concentration in the second subband, and the balance equation for the electrons occupying the bottom of the first subband (with partial concentration n_0) can be written in the form

$$\frac{n_0}{\tau_{1\rm out}} = \frac{m}{\pi\hbar^2}\int_{\varepsilon_{\rm th}}^{\Delta-\hbar\omega_{\rm ph}} {\rm d}\varepsilon_1 \frac{f(\varepsilon_1)}{\tau_{\rm pl}^{(21)}(\varepsilon_1)}. \tag{2}$$

Here $f(\varepsilon_1)$ is the electron distribution function in the first subband, normalized as

$$\frac{m}{\pi\hbar^2}\int_{\varepsilon_{\rm F}}^{\Delta-\hbar\omega_{\rm ph}} {\rm d}\varepsilon_1 f(\varepsilon_1) = n_1 - n_0,$$

$$f(\varepsilon_1 < \varepsilon_{\rm F}) = f_0 \approx \frac{\pi\hbar^2 n_0}{m\varepsilon_{\rm F}} \tag{3}$$

and $1/\tau_{\rm pl}^{(21)}$ is the electron scattering rate by intersubband plasmons. In the high-energy region, $\varepsilon_{\rm F} < \varepsilon_1 < \Delta_{21}$, the distribution function $f(\varepsilon_1)$ is established by optical phonon and intrasubband-plasmon

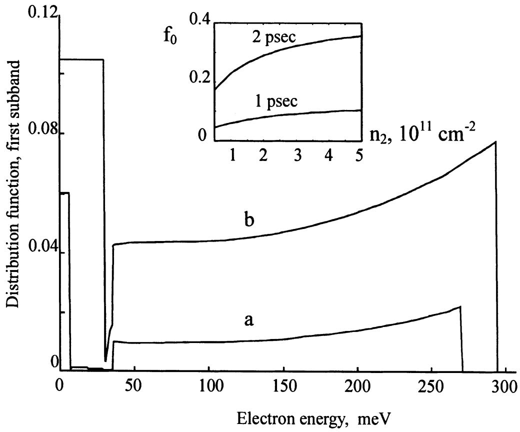

Fig. 2. Distribution function for the electron population in the first subband calculated for subband depopulation time $\tau_{1\,\mathrm{out}} = 1$ ps and two values of electron concentration n_2: (a) $1 \times 10^{11}\ \mathrm{cm}^{-2}$; (b) $5 \times 10^{11}\ \mathrm{cm}^{-2}$. The inset shows the occupation number f_0 for the bottom states in the first subband as a function of the electron concentration n_2, calculated for two different values of depopulation time $\tau_{1\,\mathrm{out}}$.

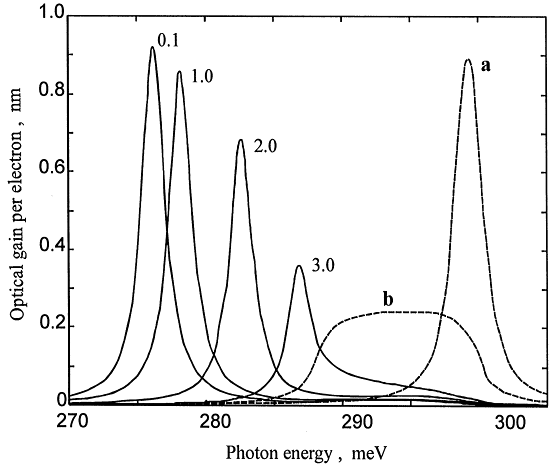

Fig. 3. Down-shift and narrowing of the optical gain spectra due to the depolarization effect calculated for the quantum well with inverted subband occupation. Dashed curves represent calculations neglecting the depolarization effect for two values of electron concentration n_2: (a) $5 \times 10^{10}\ \mathrm{cm}^{-2}$; (b) $4 \times 10^{11}\ \mathrm{cm}^{-2}$. Solid curves labeled with the value of the depopulation time $\tau_{1\,\mathrm{out}}$ (in ps) illustrate the influence of the resonance screening and first subband bottom filling on the gain spectrum at $n_2 = 4 \times 10^{11}\ \mathrm{cm}^{-2}$. The low-temperature value 1 meV was taken for the polarization dephazing rate in this calculation.

cascade emission and can be approximated by the simple expression

$$f(\varepsilon_1) \propto \exp\left(-\frac{\Delta_{21} - \hbar\omega_{\mathrm{ph}} - \varepsilon_1}{W_{11}\tau_{1\mathrm{out}}}\right), \tag{4}$$

where $W_{11} = W_{\mathrm{ph}}^{(11)} + W_{\mathrm{pl}}^{(11)}$ is the total cascade cooling rate for 1–1 intrasubband relaxation processes. For an exemplary calculation, we consider an infinitely deep quantum well of width 4 nm and subband energy separation $\Delta_{21} = 300$ meV. In this limit the mode coupling can be neglected in first approximation, and a reasonably good description of the relaxation process is possible by using only bare phonon and plasmon modes. The scattering rates, $\tau_{\mathrm{pl,ph}}^{-1}$, have been calculated for $T = 0$ K using the dielectric continuum model and material parameters of $\mathrm{Ga_{0.47}In_{0.53}As}$. Fig. 2 represents the distribution function for the electron population in the first subband calculated for subband depopulation time $\tau_{1\mathrm{out}} = 1$ ps and two values of electron concentration n_2: $a - 1{\times}10^{11}\ \mathrm{cm}^{-2}$, $b - 5{\times}10^{11}\ \mathrm{cm}^{-2}$. Two separate groups of electrons are readily seen in the first subband: "cool" electrons in the subband bottom and "hot" electrons in high-energy states characterized by the distribution function (4). The inverted population of the high-energy states is formed by cascade-like emission of optical phonons and intrasubband plasmons, whereas the subband bottom states with $k \leqslant k_{\mathrm{F}}$ are filled mostly due to the one-step events of intersubband plasmon excitation. We would like to emphasize that the latter process effectively fills precisely those states which are the final states for light-emitting transitions (states with $k \leqslant k_{\mathrm{F}}$ in the model considered here), restricting to some extent the value of inverted population. This effect becomes more pronounced if the depopulation time increases. The inset in Fig. 2 shows the occupation number f_0 for the bottom states in the first subband as a function of the electron concentration n_2, calculated for two different values of depopulation time $\tau_{1\mathrm{out}}$.

The optical characteristics of the quantum well are substantially influenced by the inter-subband plasmon spectrum due to the resonant screening of the light-wave field. In a system with normal ordering of the subband occupation this leads to an up-shift in the energy and to substantial narrowing of the inter-subband absorption spectrum [8]. Fig. 3 shows down-shift and narrowing of the optical gain spectra due to the depolarization effect calculated for the quantum well with inverted subband occupation. Dashed curves represent calculations neglecting the depolarization effect for two values of electron concentration n_2: $a - 5\times10^{10}$ cm^{-2}; $b - 4\times10^{11}$ cm^{-2}. Solid curves labeled with the value of the depopulation time $\tau_{1\mathrm{out}}$ (in ps) illustrate the influence of the resonance screening and first subband bottom filling on the gain spectrum at $n_2 = 4\times10^{11}$ cm^{-2}. The low-temperature value 1 meV was taken for the polarization dephazing rate in this calculation.

Acknowledgements

This work was supported by US Army Research Office under grant DAG55-97-1-0009.

References

[1] M.A. Stroscio, G.J. Iafrate, K.W. Kim, M.A. Littlejohn, H. Goronkin, G.N. Maracas, Appl. Phys. Lett. 59 (1991) 1093.
[2] M. Stroscio, J. Appl. Phys. 80 (1996) 6864.
[3] S. Das Sarma, in: J. Shah (Ed.), Hot Carriers in Semiconductor Nanostructures, Academic Press, New York, 1996, p. 53.
[4] L. Wendler, R. Pechstedt, Phys. Stat. Sol. B 141 (1987) 129.
[5] S.J. Allen, D.C. Tsui, B. Vinter, Solid State Commun. 20 (1976) 425.
[6] V. Gorfinkel, S. Luryi, B. Gelmont, IEEE J. Quantum Electron. 32 (1996) 1995.
[7] M. Kisin, M.A. Stroscio, G. Belenky, S. Luryi, Appl. Phys. Lett. 73 (1998) 2075.
[8] R.J. Warburton, C. Gauer, A. Wixforth, J.P. Kotthaus, B. Brar, H. Kroemer, Superlattices Microstruct. 19 (1996) 365.